Scientific Research Publishing

Open Journal of Geology, 2026, 16(5), 243-262
https://www.scirp.org/journal/ojg
ISSN Online: 2161-7589
ISSN Print: 2161-7570

Mechanisms of Emplacement and Position in the Eburnean Orogeny of the Deou Alkaline Pluton (Northern Burkina Faso)

Abraham Seydoux Traoré[1], Saga Sawadogo[1*], Oussény Sourgou[1,2], Adama Ouédraogo Yaméogo[1,3], Seta Naba[1]

[1]Geosciences and Environment Laboratory, Department of Earth Sciences, Joseph KI-ZERBO University, Ouagadougou, Burkina Faso
[2]University Center of Manga, Norbert Zongo University, Koudougou, Burkina Faso
[3]Training and Research Unit in Science and Technology, Department of Life and Earth Sciences, Norbert Zongo University, Koudougou, Burkina Faso
Email: *sawadsaga@gmail.com

How to cite this paper: Traoré, A.S., Sawadogo, S., Sourgou, O., Yaméogo, A.O. and Naba, S. (2026) Mechanisms of Emplacement and Position in the Eburnean Orogeny of the Deou Alkaline Pluton (Northern Burkina Faso). *Open Journal of Geology*, **16**, 243-262.
https://doi.org/10.4236/ojg.2026.165013

Received: March 27, 2026
Accepted: May 5, 2026
Published: May 8, 2026

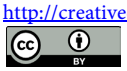

Abstract

The Deou granite belongs to the late granitoid group. Its structures are therefore important for interpreting the emplacement mechanisms and deducing the tectonic regime that prevailed at the end of the Eburnean orogeny. The aim of studying this pluton is to understand the mechanisms that prevailed at the end of the Eburnean orogeny. The petrographic and geochemical study reveals that the Deou granite is an alkaline granite belonging to the A-type. Magnetic susceptibility values show that the pluton is essentially ferromagnetic due to the presence of magnetite. Magnetic fabrications measured in the laboratory show foliations that are always steeply dipping and lineations that are steeply plunging in places. These steeply dipping lineation zones can be interpreted as the magma feed zones par excellence of the pluton. These fabrics are where the plutons are emplaced, since the microstructures observed are essentially magmatic. The fabrications of the Deou alkaline granite obtained from measurements of magnetic susceptibility anisotropy and the various geotectonic diagrams used show that the granite was emplaced in a diapiric context. This suggests anorogenic emplacement. These data confirm the post-orogenic nature of the Deou granite, which did not undergo any major reworking after emplacement.

Keywords

Deou, Eburnean, Puton, Rheology, Magnetic Fabric

1. Introduction

Granitoids make up around 70% of the bedrock of the Man/Leo Shield (**Figure 1**) [1], where the geological formations are essentially Palaeoproterozoic in age [2]-[9].

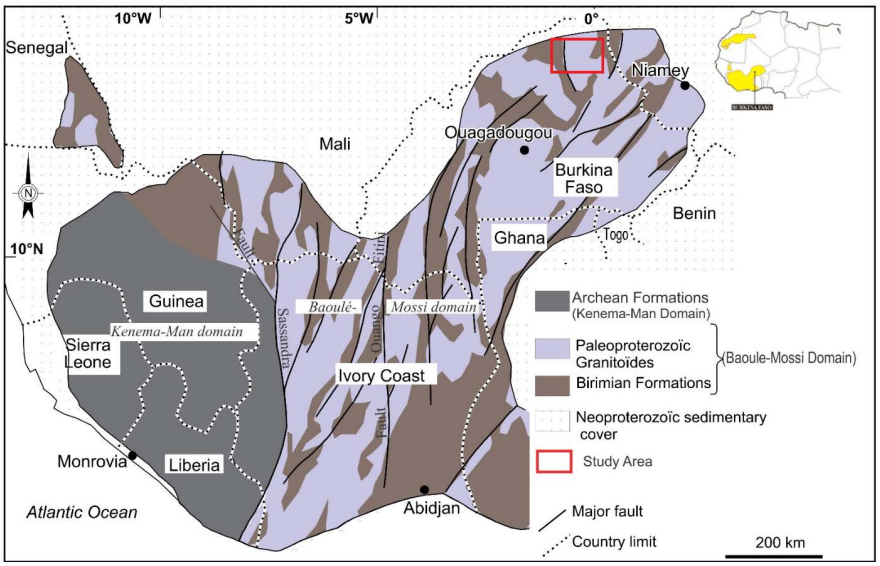

Figure 1. Simplified geological map of the Man/Leo Shield [1].

According to the radiometric ages obtained, Tonalite, Trondhjemite, and Granodiorite (TTG) granitoids and biotite granites were emplaced during the Eburnean orogeny [10]-[12], whereas alkaline granites are late and generally post-orogenic [13]-[15]. The outcrops of the latter are very discrete in the field, so most suggestions about their geodynamic contexts are based on petrographic and geochemical studies. However, a few structural studies of granites have been carried out effectively in the Man/Léo shield, notably in Niger [16] and Burkina Faso [17]-[22].

The present study focuses on the reconstruction of the emplacement mechanisms of the Deou granite pluton in northern Burkina Faso and its position in the Eburnean orogeny. This analysis of the alkaline pluton will be based on petrographic and geochemical characteristics on the one hand, and on the use of the Magnetic Susceptibility Anisotropy (MSA) technique and the examination of microstructures on the other hand.

Diapiric emplacement implies stress-free emplacement by gravitational uplift, with structures that are consistent with those of the surrounding rock and concentric foliation within the granitoid.

2. Regional Geological Context

The study area is made up of metavolcanic and metasedimentary rocks that form more or less narrow belts cut by vast batholiths of TTG-type granitoids. All the belts and the TTGs were cut at different times by second-generation granitoids,

mainly calc-alkaline [2] (**Figure 2(A)**). The first major period was between 2.150 and 2.130 Ga, with the emplacement of plutons along shear zones [12]. The second period runs from 2.117 to 2.095 Ga and corresponds to the emplacement of gigantic batholiths in the center of the country [12]. Finally, the alkaline granite and syenite plutons, which are generally small in size and are thought to have been emplaced between 1.889 and 1.819 Ga [12] [23], are considered to be completely late.

The Deou pluton (**Figure 2(B)**), the subject of this study, belongs to the latter group. The Deou granitic pluton, located between longitudes 0.60˚W and 0.80˚W and between latitudes 14.55˚N and 14.80˚N, has been mapped as an alkaline granite [24] and would therefore belong to the latter group. It is intrusive in a host rock composed of metavolcanic and metasedimentary rocks and TTGs. To the north, it is unconformably overlain by the Neoproterozoic formations of the Taoudeni basin (**Figure 2(B)**).

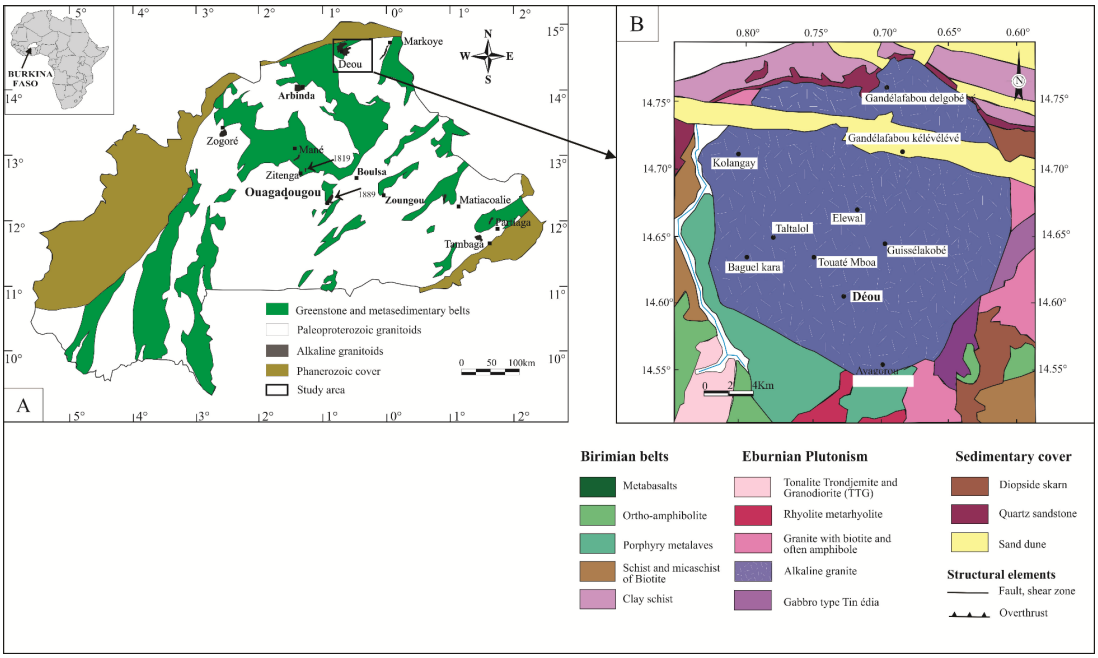

Figure 2. (A) Simplified geological map of Burkina Faso showing the study area [12]; (B) Map of the Deou pluton and its surrounding area [24].

3. Methodology

The Deou pluton was cored in the field using a portable two-stroke drill. At each sampling station, two to three cores were taken for petrographic, microstructural, geochemical, and magnetic studies. At each sampling site, which is georeferenced by coordinates (longitude, latitude) using a GPS (Global Positioning System) receiver, a minimum of two cores samples, each between 7 cm and 10 cm in length, are collected at intervals of a few meters. Before extraction, the core is oriented in azimuth, dip, and dip direction (**Figure 3(a)**). The orientation obtained is indicated by drawing an arrow and extending it along the core's generatrices; the di-

rection of the arrow indicates the dip direction (**Figure 3(b)**).

In the laboratory, the cores are cut perpendicular to their axis, taking into account the ratio h = 0.88 × d, where d is the core diameter (inner diameter of the core). This h/d ratio for a cylinder is the one that most closely approximates the shape of a sphere (**Figure 3(b)**). In practice, d ≈ 25 mm and h ≈ 22 mm. Two cylindrical samples per core are used for laboratory measurements. A total of 64 sites were sampled for magnetic susceptibility anisotropy (MSA) measurements. The majority of these sites (61) are located in the Deou pluton and the other three in the nearby host rok due to the poor quality of the outcrop within the host rock. Numerous studies have shown that the ASM fabrics are coaxial with the mineral fabrics [25] [26]. The magnetic lineation corresponds to the K1 axis of the magnetic susceptibility ellipsoid, and the K3 axis corresponds to the pole of the magnetic foliation.

The geochemistry was based on mineral analysis using the Camebax SX 50 electron microprobe at the Geosciences and Environment Laboratory in Toulouse and chemical analysis data on total rock (ALS-Chemex). The magnetic studies focused on characterising the magnetic mineralogy using CS2 and measuring the magnetic susceptibility and anisotropy of magnetic susceptibility using the Kappabridge KLY-3 in the same laboratory.

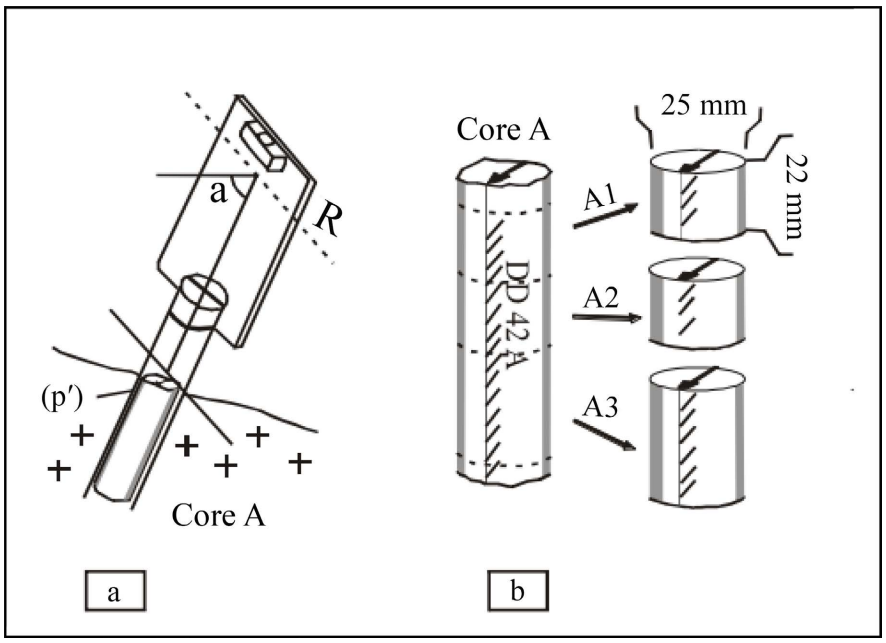

Figure 3. Sample collection procedure for ASM measurements. (a) orientation using a compass and clinometer; p is the direction of the plane perpendicular to the core axis (p'= p ± 90) and α are the azimuth and dip of the core axis; the line along the core represents the vertical plane passing through the core axis, and the arrow above the core indicates the direction of dip parallel to p'; (b) Samples A1 and A2 are collected from core A; two additional samples are collected from core B, resulting in 4 samples per site, *i.e.*, a rock volume of 4 × 10.8 cm^3; Pieces A3 and B3 may provide additional ASM samples and are also used for preparing thin sections and determining microstructures; (c) The ASM measurement provides the declination and inclination of each axis relative to the sample axes. d: Using p' and *a*, the ASM ellipsoid is calculated relative to the geographic reference frame [26].

4. Results

4.1. Petrographic Character of the Host Rock of the Deou Pluton

The host rock consists mainly of quartz sandstone and metabasalt. The quartz microdiorite is leucocratic, micrograined, and composed mainly of amphibole, biotite, plagioclase, and quartz (Figure 4(a)). The metabasalts are greenish, microlithic porphyry, containing plagioclase phenocrysts (2 mm - 4 mm) in an almost entirely chloritized matrix of amphibole and biotite (Figure 4(b)). The sandstones (Figure 4(c)) are composed mainly of quartz with a blunt edge, evidence of a slightly significant transport (Figure 4(d)), and represent a minor component.

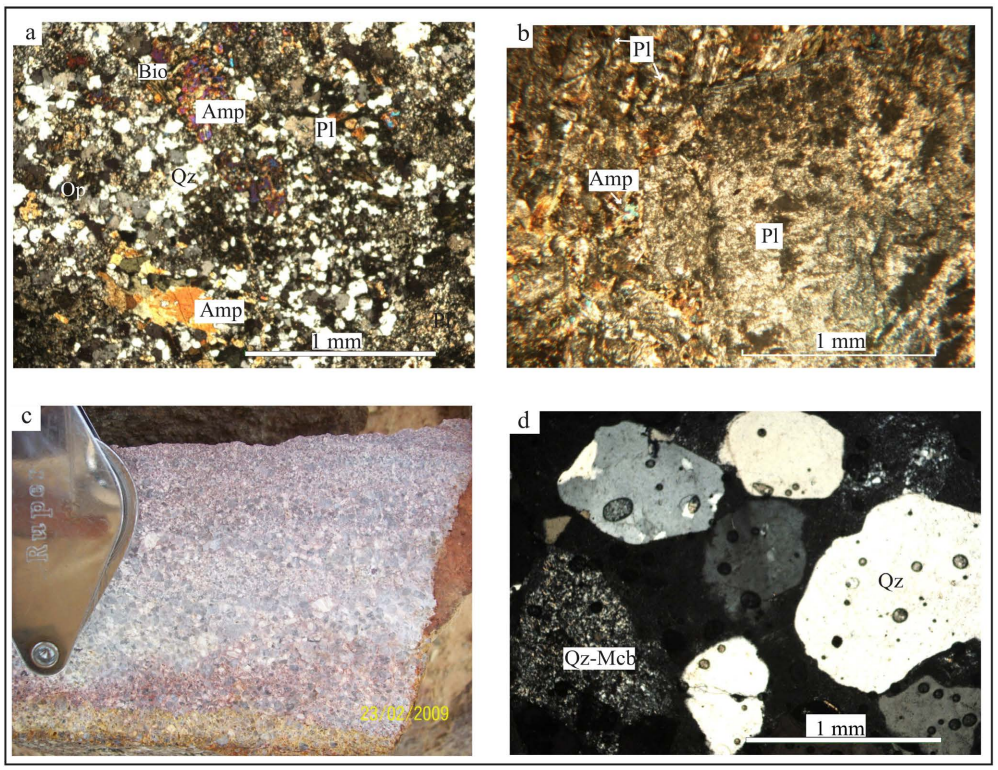

Figure 4. The main facies of the surrounding Deou granite (Amp: amphibole; Bio: biotite; Pl: plagioclase; Qz: quartz; Qz-Mcb: quartz-micas blancs; Op: opaque.)

4.2. Petrographic and Geochemical Characteristics of the Deou Pluton

4.2.1. Petrographic Characteristics of the Deou Pluton

The granite outcrops in the form of hills and is rarely flush with the ground. The rock is leucocratic with a pink heterogranular background (0.5 mm - 4 mm), but microscopic examination distinguishes a non-granophyric facies (Figure 5(a)-(c)) and a granophyric facies (Figure 5(b), Figure 5(d)), to which a rosette facies is added (Figure 5(e)). However, apart from the proportion of minerals, the mineralogical assemblage is the same for all facies: amphibole-biotite-potassium and quartz feldspars.

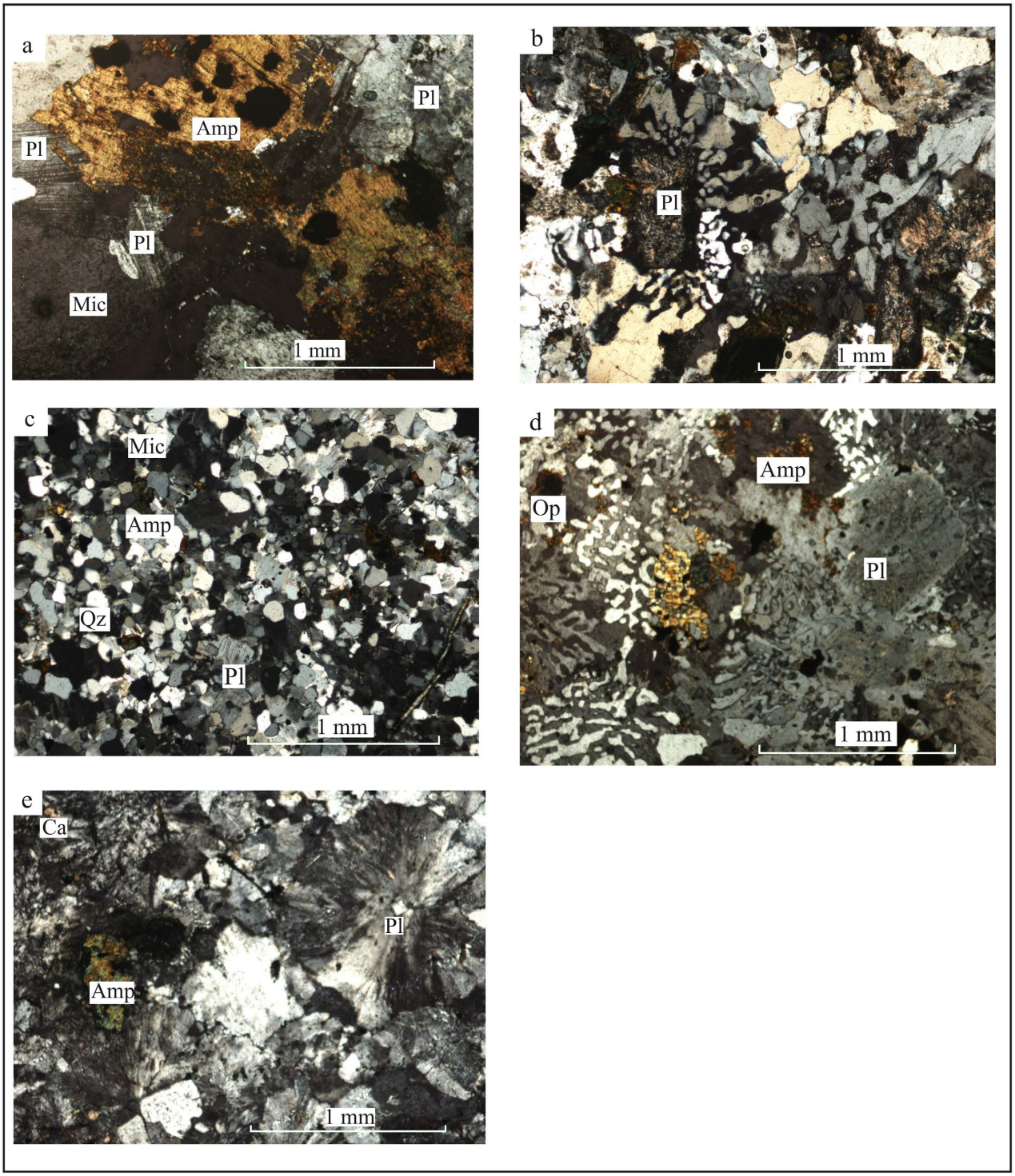

Figure 5. Main facies of the Deou granite seen under microscopy; same legend as the previous figure; (a) Non-granophyric coarse facies; (b) Granophyric coarse facies; (c) Non-granophyric fine facies; (d) Granophyric fine facies; (e) Rosette facies.

4.2.2. Geochemical Characteristics of the Deou Pluton

The Deou granite is classified as an alkaline feldspar granite in the Q-A-P [27] normative diagram (**Figure 6**). The alkaline nature of the feldspars is confirmed by geochemical data (**Figure 7**).

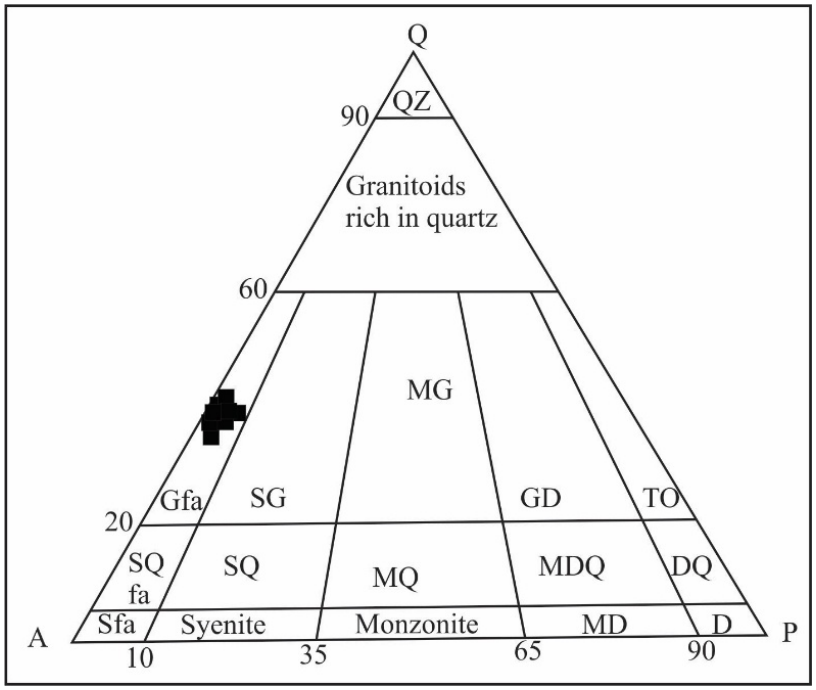

Figure 6. Diagram Q-A-P [27] showing representative facies of the Deou granite; MG: Monzogranite; GD: Granodiorites; TO: Tonalites; MDQ: Monzodiorite quartzique; DQ: Diorite quartzique; D: Diorite; MD: Monzodiorite; Sfa: Syenite à feldspath alcalin; Sqfa: Syenite quartzique à feldspath alcalin; SQ: Syenite quartzique; MQ: Monzonite quartzique; Gfa: granite à feldspath alcalin; SG: Syéno-granite; QZ: Quartzolite.

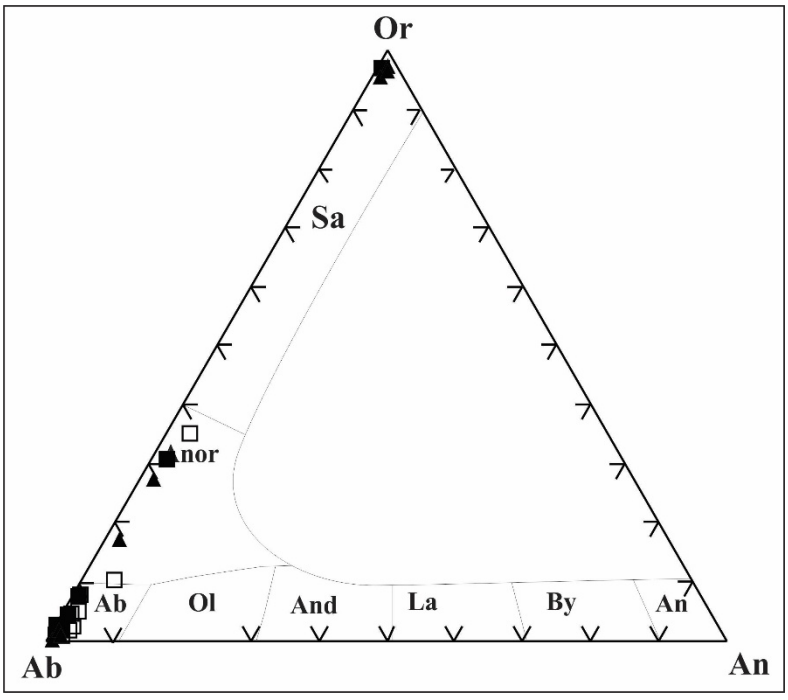

Figure 7. Composition of plagioclases in the coarse non-granophyric facies of Deou (De 72 = solid squares; De 98 = empty squares) and fine-grained granite (solid triangles = De 60) in the Or-Ab-An diagram. An = anorthite; By = bytownite; La = labrador; And = andesine; Ol = oligoclase; Ab = albite; Anor = anorthose; Sa = sanidine; Or = orthose.

It is peraluminous (A/CNK between 1.29 and 1.39) (Figure 8), siliceous (74 < SiO_2 < 77), sodi-potassic (7 < $Na_2O + K_2O$ < 9) with moderate CaO (0.51 - 1.13), Fe2O3 (1.7 - 3.67), and MgO (0.02 - 0.16) contents (Table 1). Zr, Nb, Y, Ga, Ce, and Ta contents are high, with Zr + Nb + Ce + Y > 400 ppm, typical of alkaline granites, while the Eu anomaly (Eu/Eu* < 0.7) remains negative, reflecting the depletion of residual plagioclase or alkaline feldspar. In the diagrams [28], it unambiguously occupies the domain of type A granites (Figure 9).

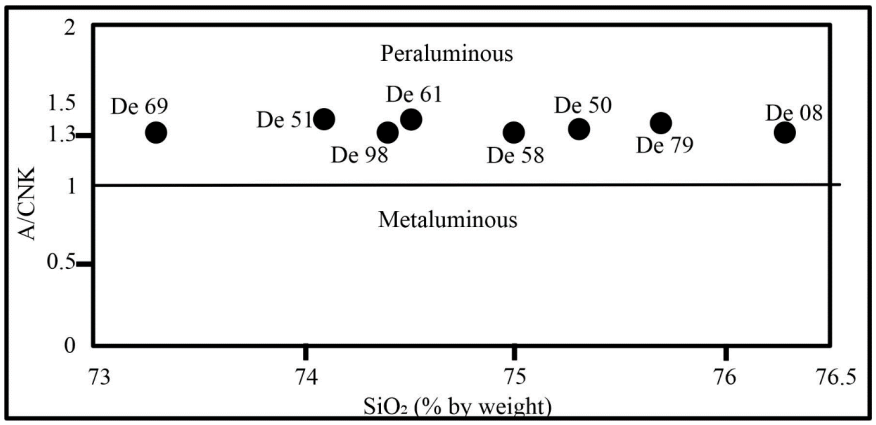

Figure 8. Chemical discrimination in the A/CNK diagram [$Al_2O_3/(CaO + Na_2O + K_2O)$] as a function of SiO_2 in the Deou granite.

Table 1. Analytical and normative data on the total rocks of the Deou granite.

Samples	De 79	De 98	De 50	De 58	De 08	De 51	De 61	De 69
Petrography	Non-granophyric coarse facies	Non-granophyric coarse facies	Coarse granophyric facies	Coarse granophyric facies	Non-granophyric coarse facies	Granophyric aplitic facies	Rosette-like aplitic facies	Rosette-like aplitic facies
Major elements (%)								
SiO_2	75.7	74.4	75.3	75	76.3	74.1	74.5	73.3
TiO_2	0.15	0.15	0.14	0.27	0.21	0.28	0.26	0.22
Al_2O_3	11.55	11.85	11.15	11.75	10.75	11.55	11.05	11.3
Fe_2O_3	1.7	1.69	1.82	3.62	2.18	3.67	3.18	2.91
MnO	0.04	0.03	0.05	0.08	0.05	0.07	0.08	0.06
MgO	0.07	0.16	0.06	0.06	0.07	0.06	0.12	0.02
CaO	0.51	0.64	0.45	1.13	0.61	0.96	0.63	0.92
Na_2O	3.68	3.58	3.83	4.24	3.81	4.07	4.27	4.09
K_2O	4.62	4.78	3.97	3.61	3.92	3.26	3.21	3.55
$Na_2O + K_2O$	8.3	8.36	7.8	7.85	7.73	7.33	7.48	7.64
P_2O_5	0.02	0.02	0.02	0.03	0.01	0.02	<0.01	0.01
LOI	1.1	1.58	0.8	0.89	0.79	1.96	1.69	1.38
Total	99.2	98.88	97.7	100.68	98.9	100	99.1	98.76
A/CNK (mol.)	1.31	1.32	1.35	1.31	1.29	1.39	1.36	1.32

Continued

Normes (%)								
Q	34.89	33.92	38.27	34.75	39.51	36.08	37.42	35.49
Or	29.06	28.25	24.26	21.33	23.68	19.27	19.51	20.98
Ab	31.1	30.29	33.44	35.88	32.89	34.44	37.09	34.61
An	2.17	2.15	1.52	2.37	0.64	3.617	1.52	1.99
C	0	0	0	0	0	0	0	0
Di Wo	0.41	0	0.18	0.84	0.21	0.244	0.36	0.77
Di en	0.35	0.38	0.15	0.32	0.18	0	0.3	0.11
Di fs	0	0.22	0	0	0	0.036	0	0
Trace elements (ppm)								
Cr	<10	<10	<10	<10	<10	<10	<10	10
Ni	2	<1	2	<1	2	<1	2	<1
Co	132	146	144	148	183	146	138	108
Ga	23.1	21.8	25.7	22	18.3	21.8	22	23.4
V	11	5	<5	<5	<5	<5	11	<5
Pb	12	20	13	10	<2	9	4	8
Rb	164.5	156	144.5	85.9	75.8	76.3	94.1	101.5
Cs	3.95	3.15	1.95	0.98	0.19	0.76	0.84	1.51
Ba	785	736	607	742	1435	908	933	732
Sr	32.1	45.4	43.5	89.9	35.6	110	90.2	84.6
Ta	1.4	1.4	2.3	1	0.7	0.8	1.1	1.4
Nb	17.2	17.2	25.3	14.7	10.3	13.7	15.3	18.2
Hf	9.5	8.8	11	13.6	9.3	13.8	14.1	13.9
Zr	303	256	310	508	365	530	534	509
Y	68.6	63.8	102	81.4	58.2	87.6	93.8	84.9
Th	5.9	5.97	7.73	5.43	3.29	5.1	5.59	6.14
U	2.22	2.73	2.74	1.88	0.86	1.72	1.97	2.32
Zn	151	163	147	124	80	116	111	141
Cu	9	9	<1	4	<1	3	<1	2
W	708	796	700	826	931	807	717	587
Sn	4	12	4	3	1	2	4	3
Sb	0.24	0.48	0.18	<0.05	<0.05	0.08	<0.05	0.12
Samples	De 79	De 98	De 50	De 58	De 08	De 51	De 61	De 69
Rare earths elements(ppm)								
La	43.7	36.2	44.7	39	34.3	43.6	62.7	43.6
Ce	92.9	77	111	87.6	78.8	90.8	124	93.1
Pr	12.2	10.05	12.8	11.35	10.75	12.35	17.95	12.2
Nd	48.5	40.6	52.5	46.1	45.2	51	73.2	49.9
Sm	11.45	10.05	12.95	11.5	10.55	12.55	16.95	12.4

Continued

Eu	1.7	1.4	2.37	2.5	1.95	2.8	3.95	2.73
Gd	12.5	10.4	15.2	12.95	11.5	14.2	19	13.3
Tb	2.1	1.8	2.85	2.29	1.95	2.49	3.14	2.39
Dy	12.3	11.2	17.5	14.1	11.35	15	18.25	14.9
Ho	2.54	2.37	3.8	2.99	2.35	3.16	3.84	3.19
Er	7.86	7.27	11.45	9.09	6.63	9.3	11	9.58
Tm	1.11	1.1	1.71	1.33	0.95	1.32	1.6	1.41
Yb	7.28	7.16	10.7	8.65	5.91	8.37	9.97	9.38
Lu	1.1	1.1	1.65	1.28	0.92	1.26	1.49	1.4
Y + Ce + Zr + Nb	481.7	414	548.3	691.7	512.3	722.1	767.1	705.2
ΣREE	257.24	217.7	301.18	250.73	223.11	268.2	367.04	269.48
(La/Yb)N	4.8	4.04	3.34	3.61	4.64	4.17	5.03	3.72
Eu/Eu*	0.43	0.42	0.52	0.62	0.54	0.64	0.67	0.65

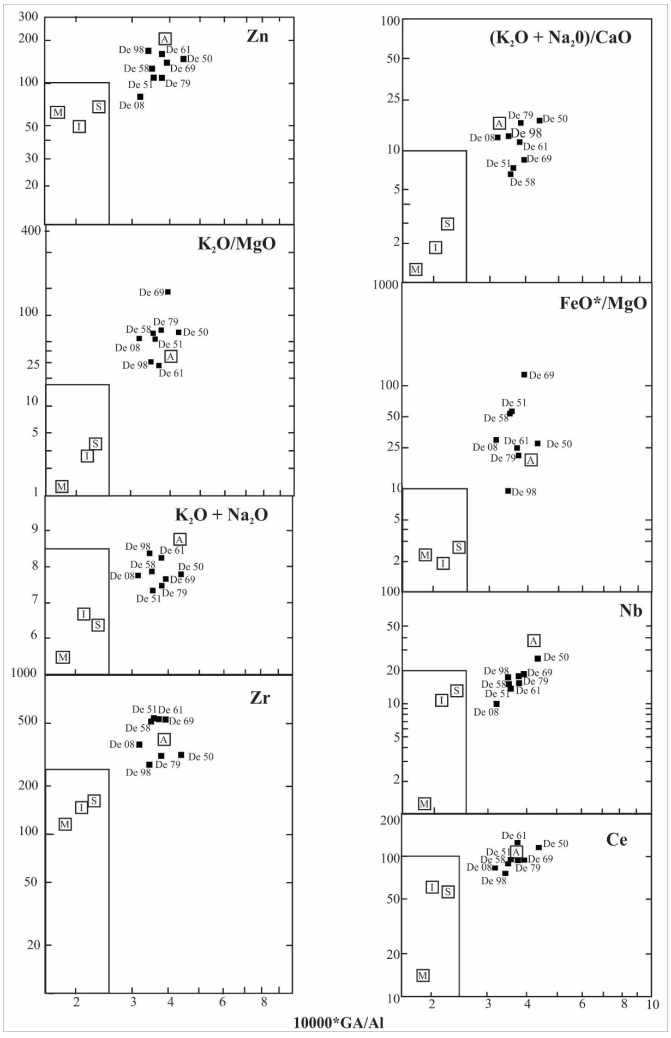

Figure 9. Discrimination diagram between I, S, M-type and A-type, in which the Deou granite is plotted [28].

4.3. Microstructures

Microscopically, almost all the microstructures of the Deou pluton are acquired in the magmatic state, marked by ± lobate quartz, free from any trace of recrystallisation, and automorphic feldspars (Figure 10(a)~(b)). This once again confirms the late-tectonic nature of the Deou pluton. Only a few sites show a low-temperature solid-state microstructure, marked by quartz banding with sub-grain recrystallisation at the edges of the large crystals, giving rise to a "core and mantle" type structure (Figure 10(c)), which is the expression of weak deformation that sometimes occurs at the end of crystallisation in any plutonic massif.

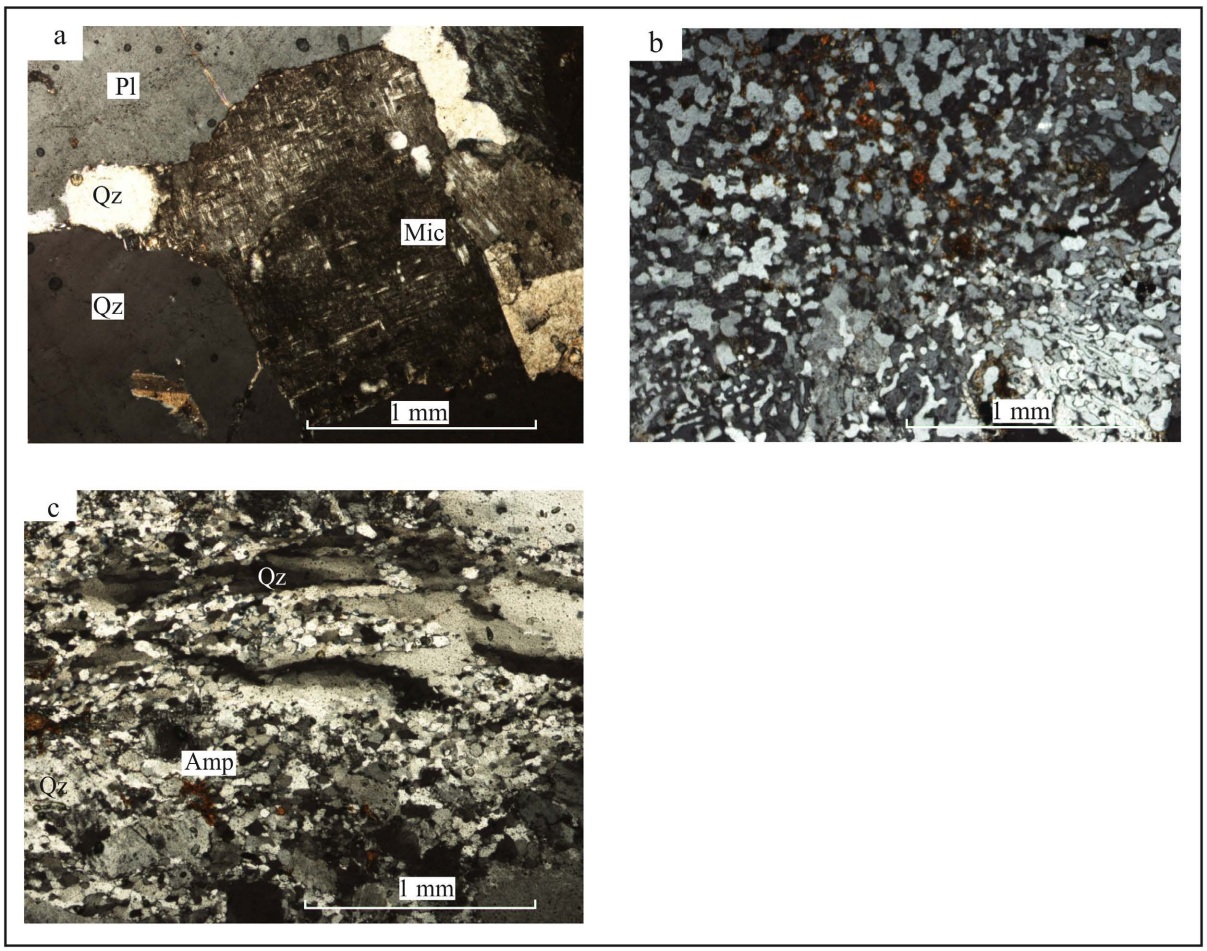

Figure 10. Microstructures of the Deou alkaline granite; same legend as the previous figure.

4.4. Magnetic and Structural Characteristics

4.4.1. Scalar Data for Magnetic Susceptibility and Thermomagnetism

At the scale of the pluton, susceptibility has a random map distribution (Figure 11), as already observed by other authors on granitic plutons in Burkina Faso [17]-[22]. This is due to the presence of magnetite, as can be seen from the various thermomagnetic curves (Figure 12), where there is a sudden drop in temperature at 580˚C, characteristic of this mineral.

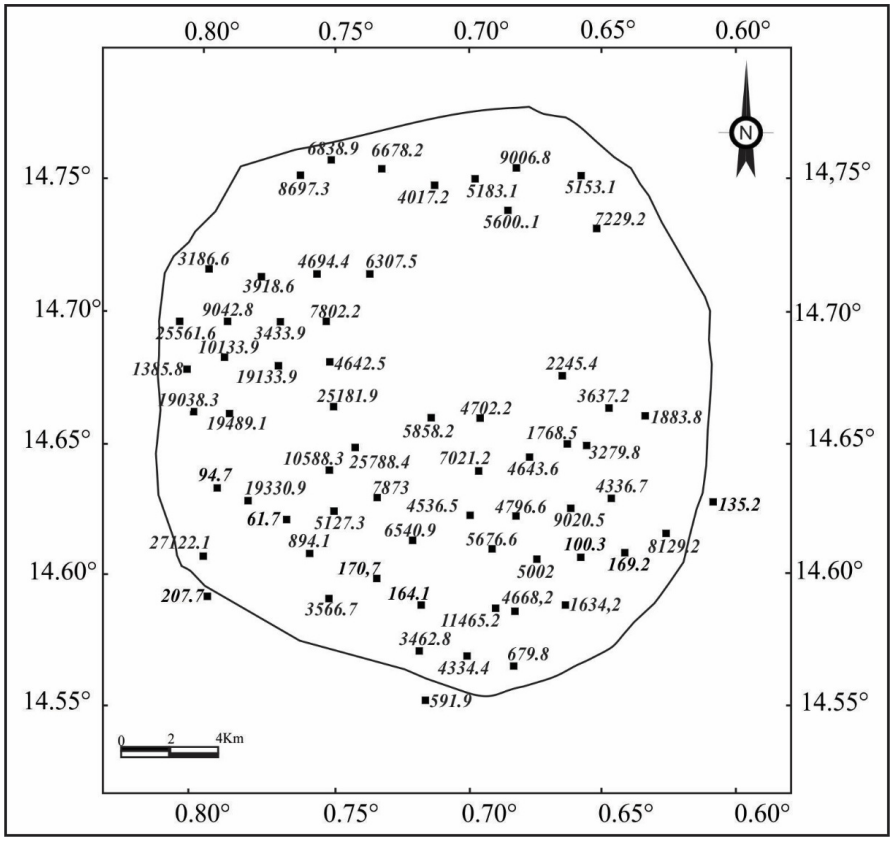

Figure 11. Map of the magnetic susceptibility (km in μSI) of the Deou alkaline granite and its surrounding area.

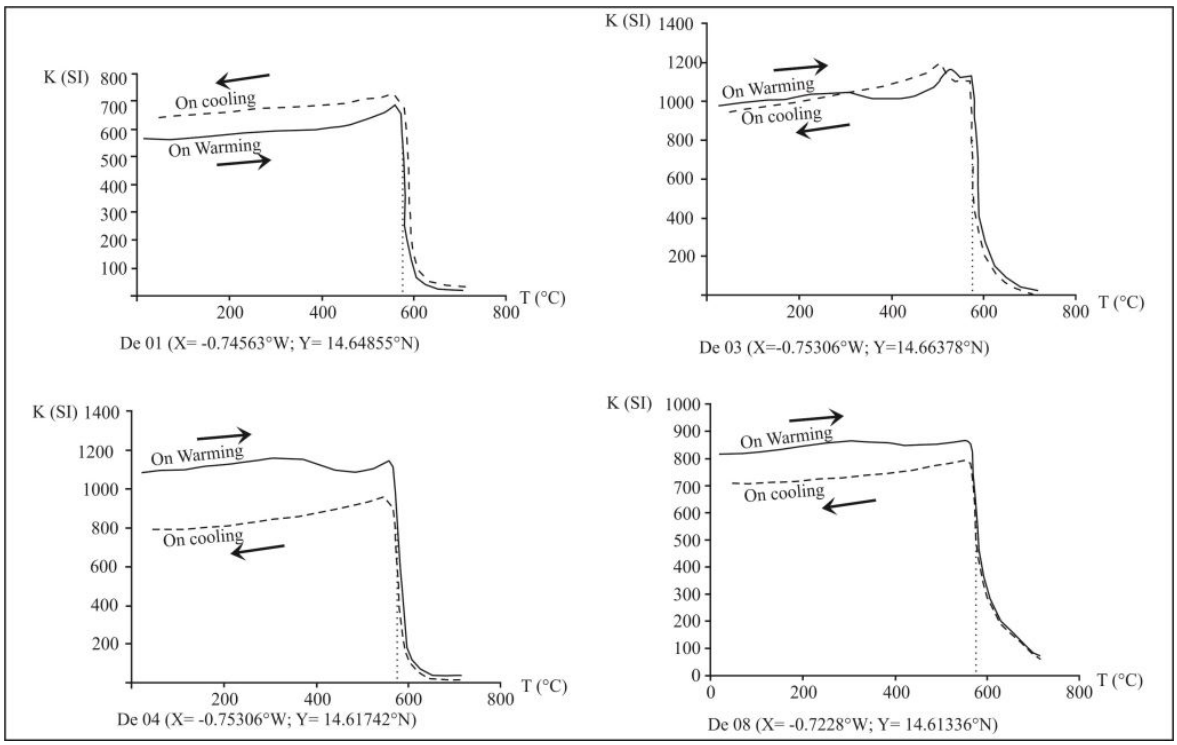

Figure 12. Thermomagnetic curves for several sampling sites in the Deou alkaline granite.

4.4.2. Directional Magnetic Susceptibility Data and Structural Analysis

1. Magnetic Foliation

The general shape of the foliation is more or less concentric, although some sites show foliations that are completely secant or even almost orthogonal to this general layout (Figure 13). The foliation of the host rock is completely secant to that of the pluton. The internal foliations of the pluton, which are discordant with the others, probably correspond to the planar fabrications of the late-magmatic veins. It is at these sites that the textures are granophyric.

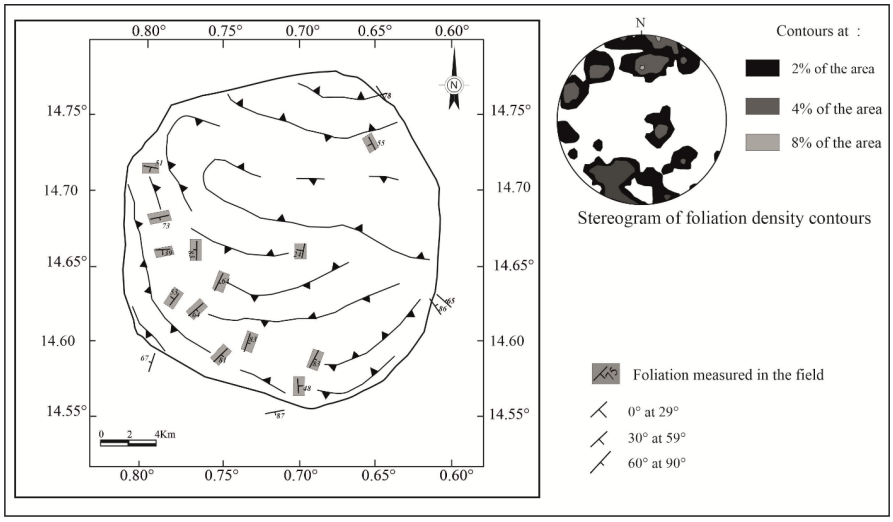

Figure 13. Map of foliations and stereograms of density contours of the Deou alkaline granite.

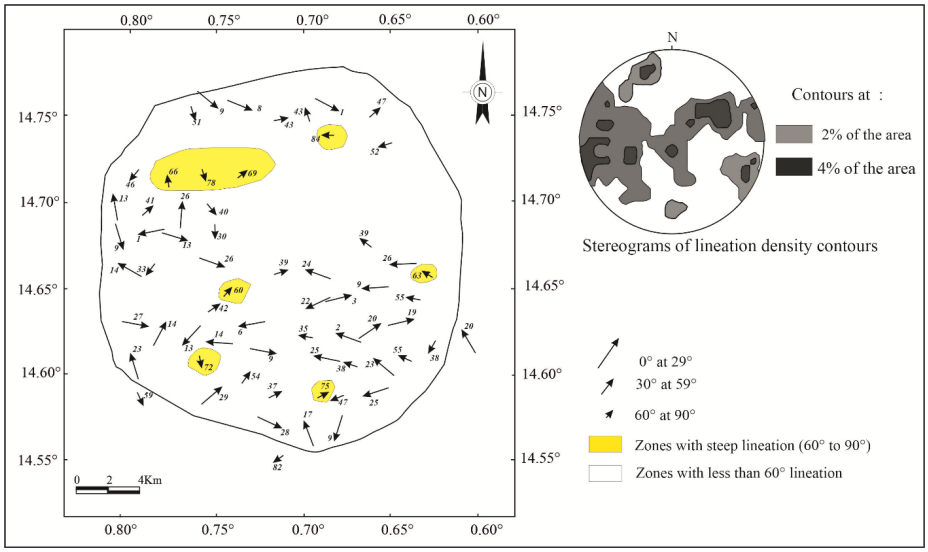

Figure 14. Lineation map and stereogram of the density contours of the Deou alkaline granite.

2. Magnetic Lineation

For lineation, the dip is considered shallow for values ≤ 30˚, moderate for values between 30˚ and 60˚, and steep for dips ≥ 60˚. The azimuths of the lineations

roughly follow the directions of the foliations, with low to medium plunges, except for a few sites (12%) where the lineations are sub-vertical (plunge ≥ 60˚) (**Figure 14**). These zones of high plunge are interpreted as pluton-feeding zones [17] [29] [30] while the zones of medium plunge reflect the finite extension of the magma at the time of crystallization [17] [29] [30]. In our case, this direction would be WNW-ESE to W-E, which is one of the directions followed by certain late fractures in the Deou zone.

5. Discussion

5.1. Setting Up Conditions

The sub-circular Deou pluton outcrops in a host rock composed of metavolcanic and metasedimentary rocks and TTG-type granitoids. It is unconformably overlain by Neoproterozoic quartz sandstones to the north. Petrogeochemical analyses (**Figure 5**) show that this is indeed an alkaline granite. Furthermore, the plagioclases in the various facies consist entirely of albite (**Figure 6**). Whose granophyric texture argues in favour of this and also indicates emplacement at a relatively high level in the crust [31]-[33]. The formation of this texture is interpreted as the result of eutectic crystallisation of a water-rich silicate magma that underwent rapid cooling [34] [35].

The pluton feed zones are somewhat scattered at this scale, but the most extensive is in the north. The low plunge values, indicating the direction of magma flow, give a WNW-ESE to W-E direction.

5.2. Positioning in the Eburnean Orogeny

Studies conducted on the Dori granitoids in north-eastern Burkina [22] and at Bouabou in south-eastern Burkina [36] show that the orientation of their foliation is concentric, indicating diapiric emplacement. However, their elliptical shape, the concordance of their foliation with their host rock, and the presence of solid-state deformation microstructures in their vicinity suggest that this diapirism is driven by regional tectonics.

In the Déou area, the structure (foliation and lineation) inferred from measurements of magnetic susceptibility anisotropy is predominantly magmatic and is therefore linked to the mechanisms that prevailed during the emplacement of the Deou granite pluton. As the foliation is concentric, this is characteristic of diapiric bodies formed in anorogenic or orogenic settings [7] [37]. In the specific case of the Deou pluton, the context would appear to be anorogenic since the few structures measured in the host rock are discordant with that of the pluton (**Figure 13**). Furthermore, the fact that it belongs to the A-type granite group indicates that the Deou granite is either anorogenic or was emplaced in a context of extension [38]. This post-orogenic character is also confirmed by the position of the Deou granite in the geotectonic classification diagram [39]. In this diagram, the Deou granite is positioned in the compositional range of post-orogenic to anorogenic granites (**Figure 15**).

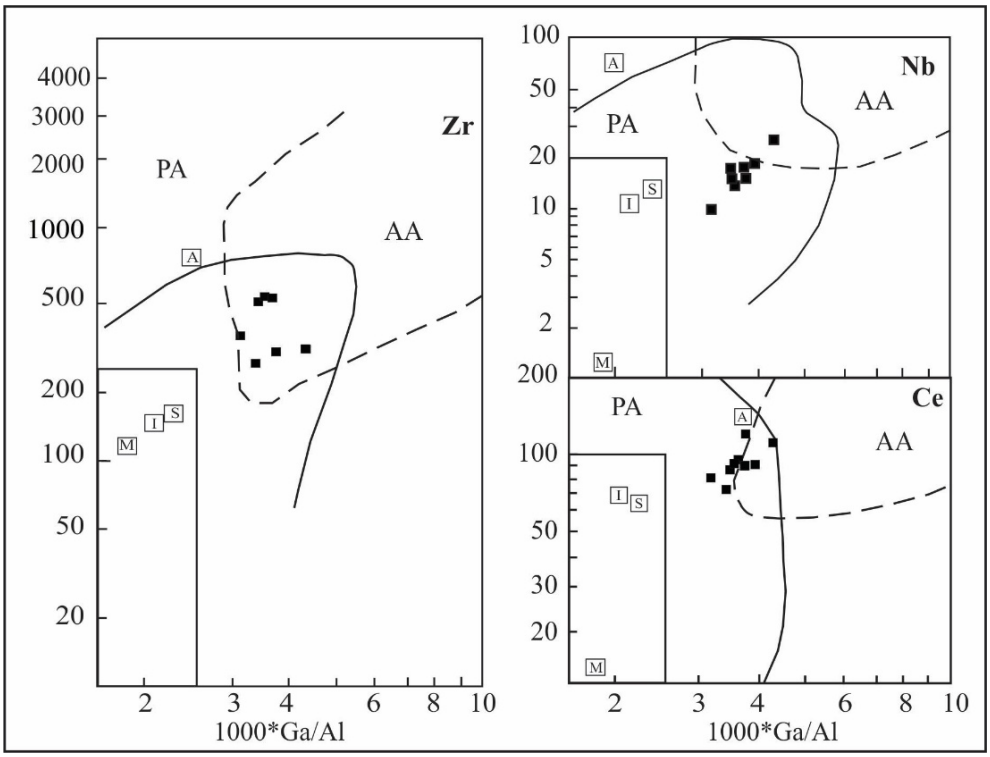

Note: A: anorogenic alkaline granite; PA: post-orogenic alkaline granite.

Figure 15. Geochemical discrimination diagram of the Deou alkaline granite [39].

Diagrams [40] [41] (**Figure 16** and **Figure 17**) show that all the samples are in the field of intra-plate granites. This confirms their position at the end of the orogeny.

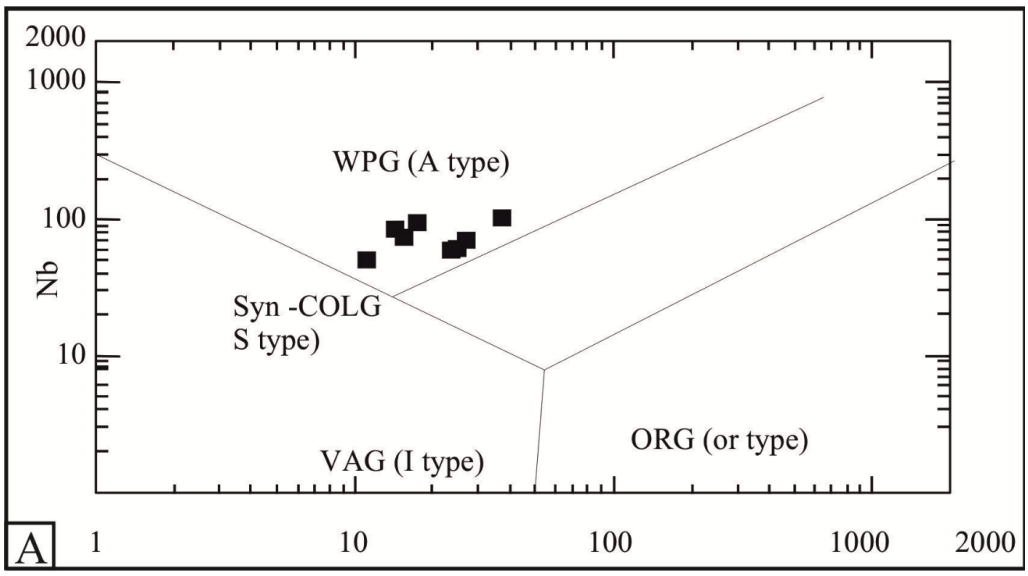

Figure 16. Geotectonic characterization diagram [40].

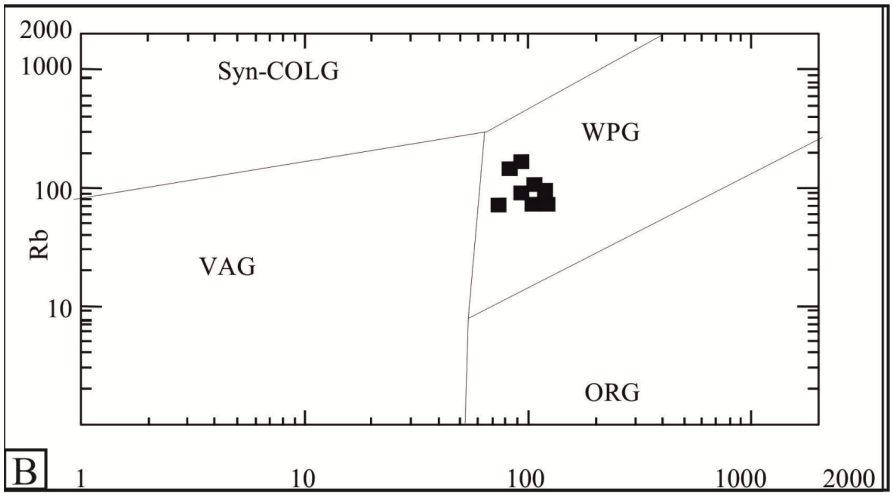

Figure 17. Geotectonic characterization diagram [41].

Based on these data, we can propose the following model for the emplacement of the Deou granite (**Figure 18**).

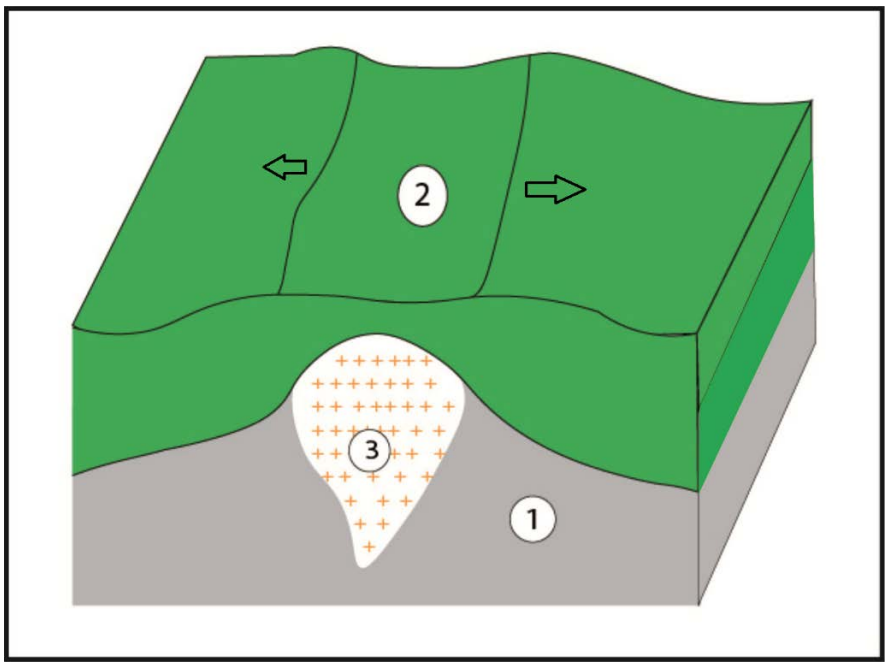

Note: 1: Lithospheric mantle; 2: Volcanic metalaves; 3: Deou granite.

Figure 18. Depositional model of the Deou alkaline granite.

6. Conclusion

The Deou granite is a heterogeneous alkaline granite. It is a peraluminous type A. The concentric fabrication of the Deou granite, coupled with the unconformity between the foliations of the pluton and the host rock, indicates diapiric emplacement in an anorogenic context. This suggests that the alkaline Deou granite was emplaced after the paroxysmal episode of the Eburnean orogeny.

Acknowledgements

The authors would like be grateful to AMIRA International and the industry sponsors for their support of the WAXI-2 Project (P934A). We are grateful to the Institut de Recherche pour le Developpement (IRD) for the logistical support for the field work. The authors also are grateful to the anonymous referees who help to improve this paper by their pertinent reviews.

Conflicts of Interest

The authors declare no conflicts of interest regarding the publication of this paper.

References

[1] Feybesse, J., Billa, M., Guerrot, C., Duguey, E., Lescuyer, J., Milesi, J., *et al.* (2006) The Paleoproterozoic Ghanaian Province: Geodynamic Model and Ore Controls, Including Regional Stress Modeling. *Precambrian Research*, **149**, 149-196. https://doi.org/10.1016/j.precamres.2006.06.003

[2] Bonhomme, M. (1962) Contribution à l'étude géochronologique de la plateforme de l'Ouest Africain. Ph.D. Thesis, Université Clermont-Ferrand, 62 p. https://www.scirp.org/reference/referencespapers?referenceid=3274945

[3] Bessoles, B. (1977) Géologie de l'Afrique. Le craton ouest-africain. Mémoires BRGM, 1-88. https://ccfr.bnf.fr/portailccfr/jsp/index_view_direct.jsp?record=bmr:UNIMARC:11437181

[4] Milési, J., Ledru, P., Feybesse, J., Dommanget, A. and Marcoux, E. (1992) Early Proterozoic Ore Deposits and Tectonics of the Birimian Orogenic Belt, West Africa. *Precambrian Research*, **58**, 305-344. https://doi.org/10.1016/0301-9268(92)90123-6

[5] Boher, M., Abouchami, W., Michard, A., Albarede, F. and Arndt, N.T. (1992) Crustal Growth in West Africa at 2.1 Ga. *Journal of Geophysical Research*: *Solid Earth*, **97**, 345-369. https://doi.org/10.1029/91jb01640

[6] Kouamélan, A.N. (1996) Géochronologie et géochimie des formations archéennes et protérozoïques de la dorsale de Man en Côte d'Ivoire. Implications pour la transition Archéen-Protérozoïque. Thèse de doctorat, Université de Rennes 1, 284 p.

[7] Lompo, M. (2010) Paleoproterozoic Structural Evolution of the Man-Leo Shield (West Africa). Key Structures for Vertical to Transcurrent Tectonics. *Journal of African Earth Sciences*, **58**, 19-36. https://doi.org/10.1016/j.jafrearsci.2010.01.005

[8] West Markwitz, V., Hein, K.A.A., Jessell, M.W. and Miller, J. (2016) Metallogenic Portfolio of the West Africa Craton. *Ore Geology Reviews*, **78**, 558-563.

[9] Salah, I.A., Liegeois, J. and Pouclet, A. (1996) Evolution d'un arc insulaire océanique birimien précoce au Liptako nigérien (Sirba): Géologie, géochronologie et géochimie. *Journal of African Earth Sciences*, **22**, 235-254. https://doi.org/10.1016/0899-5362(96)00016-4

[10] Hirdes, W., Davis, D.W., Lüdtke, G. and Konan, G. (1996) Two Generations of Birimian (Paleoproterozoic) Volcanic Belts in Northeastern Côte d'Ivoire (West Africa): Consequences for the 'Birimian Controversy'. *Precambrian Research*, **80**, 173-191. https://doi.org/10.1016/s0301-9268(96)00011-3

[11] Doumbia, S., Pouclet, A., Kouamelan, A., Peucat, J.J., Vidal, M. and Delor, C. (1998) Petrogenesis of Juvenile-Type Birimian (Paleoproterozoic) Granitoids in Central Côte-d'Ivoire, West Africa: Geochemistry and Geochronology. *Precambrian Re-*

search, **87**, 33-63.

[12] Castaing, C., Billa, M., Milési, J.P., Thiéblemont, D., Le Métour, J., Egal, E., *et al.* (2003) ANTEA 2003—Notice explicative de la carte géologique et minière du Burkina Faso à 1/1 000 000. BRGM, 147 p.

[13] Rocci, G., Bronner, G. and Deschamps, M. (1991) Crystalline Basement of the West African Craton. In: Dallmeyer, R.D., Lécorché, J.P., Eds., *The West African Orogens and Circum-Atlantic Correlatives*, Springer, 31-61. https://doi.org/10.1007/978-3-642-84153-8_3

[14] Morel, B. and Alinat, M. (1993) Géologie, pétrologie et géochimie des syénites de Ninakri: Comparaison avec d'autres massifs syénitiques anorogéniques de Côte d'Ivoire et d'Afrique de l'Ouest. *Journal of African Earth Sciences* (*and the Middle East*), **17**, 213-223. https://doi.org/10.1016/0899-5362(93)90037-q

[15] Kahoui, M. and Mahdjoub, Y. (2004) An Eburnian Alkaline-Peralkaline Magmatism in the Reguibat Rise: The Djebel Drissa Ring Complex (Eglab Shield, Algeria). *Journal of African Earth Sciences*, **39**, 115-122. https://doi.org/10.1016/j.jafrearsci.2004.07.057

[16] Pons, J., Barbey, P., Dupuis, D. and Léger, J.M. (1995) Mechanisms of Pluton Emplacement and Structural Evolution of a 2.1 Ga Juvenile Continental Crust: The Birimian of Southwestern Niger. *Precambrian Research*, **70**, 281-301. https://doi.org/10.1016/0301-9268(94)00048-v

[17] Naba, S., Vegas, N., Bouchez, J.L., Siqueira, R. and Lompo, M. (2006) Caractères magnétiques, fabriques et contexte géodynamique des granites du Burkina Faso oriental: Les plutons de Tenkodogo-Yamba, de Kouare et de Nanemi. *Africa Geoscience Review*, **13**, 63-76.

[18] Vegas, N., Naba, S., Bouchez, J.L. and Jessell, M. (2007) Structure and Emplacement of Granite Plutons in the Paleoproterozoic Crust of Eastern Burkina Faso: Rheological Implications. *International Journal of Earth Sciences*, **97**, 1165-1180. https://doi.org/10.1007/s00531-007-0205-z

[19] Traoré, A.S., Naba, S., Kagambèga, N., Lompo, M., Baratoux, L. and Ganne, J. (2011) Mise en place tardi-orogénique de la syénite de Wayen (Burkina Faso, Afrique de l'ouest). *Journal des Sciences et Technologies*, **9**, 33-48.

[20] Ilboudo, H., Sawadogo, S., Naba, S., Traoré, A.S. and Lompo, M. (2013) Structure et mode de mise en place du pluton granitique de Tiébélé et son implication dans la concentration des anomalies en Or (Au) et métaux de base (Cu-Pb-Zn), Burkina Faso (Afrique de l'Ouest). *Bulletin de l'Institut Scientifique*, *Rabat*, *Section Sciences de la Terre*, No. 35, 63-75.

[21] Sawadogo, S., Naba, S., Ilboudo, H., Traoré, A.S., Nakolendoussé, S. and Lompo, M. (2018) The Belahourou Granite Pluton (Djibo Greenstone Belt, Burkina Faso): Emplacement Mechanism and Implication for Gold Mineralization along a Shear Zone. *Journal of African Earth Sciences*, **148**, 59-68. https://doi.org/10.1016/j.jafrearsci.2018.04.009

[22] Yaméogo, A.O., Ouiya, P., Traoré, A.S., Sawadogo, S., Naba, S., Rousse, S., *et al.* (2023) Rheological Context of Emplacement of the Dori, Gorom-Gorom and Touka Bayèl Granitic Plutons (Northeast Burkina Faso, West African Craton). *Journal of African Earth Sciences*, **208**, Article ID: 105081. https://doi.org/10.1016/j.jafrearsci.2023.105081

[23] Wenmenga, U. (1986) Pétrologie des ensembles lithologiques du Protérozoïque inférieure au NE de Ouagadougou (Burkina Faso—Craton Ouest Africain). Etude pétrographique, géochimique et géochronologique. Ph.D. Thesis, Université Blaise

PASCAL Clermont-Ferrand II en France, 275 p.
http://pascal-francis.inist.fr/vibad/index.php?action=getRecordDetail&idt=8124150

[24] Delfour, J. and Jeambrun, M. (1970) Notice explicative de la carte géologique au 1/200 000 de l'Oudalan. B.R.G.M., 58 p.

[25] Borradaile, G.J. and Henry, B. (1997) Tectonic Applications of Magnetic Susceptibility and Its Anisotropy. *Earth-Science Reviews*, **42**, 49-93. https://doi.org/10.1016/s0012-8252(96)00044-x

[26] Bouchez, J.L. (1997) Granite Is Never Isotropic: An Introduction to AMS Studies of Granitic Rocks. In: Bouchez, J.L., Hutton, D.H.W. and Stephens, W.E., Eds., *Granite: From Segregation of Melt to Emplacement Fabrics*, Springer, 95-112. https://doi.org/10.1007/978-94-017-1717-5_6

[27] Streckeisen, A. (1976) To Each Plutonic Rock Its Proper Name. *Earth-Science Reviews*, **12**, 1-33. https://doi.org/10.1016/0012-8252(76)90052-0

[28] Whalen, J.B., Currie, K.L. and Chappell, B.W. (1987) A-Type Granites: Geochemical Characteristics, Discrimination and Petrogenesis. *Contributions to Mineralogy and Petrology*, **95**, 407-419. https://doi.org/10.1007/bf00402202

[29] Vigneresse, J.L. and Bouchez, J.L. (1997) Successive Granitic Magma Batches during Pluton Emplacement: The Case of Cabeza De Araya (Spain). *Journal of Petrology*, **38**, 1767-1776. https://doi.org/10.1093/petroj/38.12.1767

[30] Améglio, L., Vigneresse, J.L. and Bouchez, J.L. (1997) Granite Pluton Geometry and Emplacement Mode Inferred from Combined Fabric and Gravity Data. In: Bouchez, J.L., Hutton, D.H.W. and Stephens, W.E., Eds., *Granite: From Segregation of Melt to Emplacement Fabrics*, Springer, 199-214. https://doi.org/10.1007/978-94-017-1717-5_13

[31] Bonin, B. (2007) A-Type Granites and Related Rocks: Evolution of a Concept, Problems and Prospects. *Lithos*, **97**, 1-29. https://doi.org/10.1016/j.lithos.2006.12.007

[32] Thomas, R. and Davidson, P. (2016) Origin of Miarolitic Pegmatites in the Königshain Granite/Lusatia. *Lithos*, **260**, 225-241. https://doi.org/10.1016/j.lithos.2016.05.015

[33] Youssouf, A.Y. (2018) Origine des granophyres du Complexe du Lac Doré (CLD) et minéralisations associées, région de Chibougamau, Sous-province de l'Abitibi (Québec). Master's Thesis, Université du Québec à Chicoutimi, 186 p.

[34] Dunham, A.C. (1965) The Nature and Origin of the Groundmass Textures in Felsites and Granophyres from Rhum, Inverness-shire. *Geological Magazine*, **102**, 8-23. https://doi.org/10.1017/s0016756800053838

[35] Barker, D.S. (1970) Compositions of Granophyre, Myrmekite, and Graphic Granite. *Geological Society of America Bulletin*, **81**, 3339-3350. https://doi.org/10.1130/0016-7606(1970)81[3339:cogmag]2.0.co;2

[36] Ouédraogo, A. (2013) Études pétrostructurales du granite de Bouabou, feuille Diapaga, Sud-est Burkina Faso. Mémoire de DEA, Université de Ouagadougou, 65p.

[37] Vidal, M., Gumiaux, C., Cagnard, F., Pouclet, A., Ouattara, G. and Pichon, M. (2009) Evolution of a Paleoproterozoic "Weak Type" Orogeny in the West African Craton (Ivory Coast). *Tectonophysics*, **477**, 145-159. https://doi.org/10.1016/j.tecto.2009.02.010

[38] Barbarin, B. (1999) A Review of the Relationships between Granitoid Types, Their Origins and Their Geodynamic Environments. *Lithos*, **46**, 605-626. https://doi.org/10.1016/s0024-4937(98)00085-1

[39] Dawei, H., Shiguang, W., Baofu, H. and Manyuan, J. (1996) Post-Orogenic Alkaline

Granites from China and Comparisons with Anorogenic Alkaline Granites Elsewhere. *Journal of Southeast Asian Earth Sciences*, **13**, 13-27. https://doi.org/10.1016/0743-9547(96)00002-5

[40] Pearce, J.A., Harris, N.B.W. and Tindle, A.G. (1984) Trace Element Discrimination Diagrams for the Tectonic Interpretation of Granitic Rocks. *Journal of Petrology*, **25**, 956-983. https://doi.org/10.1093/petrology/25.4.956

[41] Pearce, J. (1996) Sources and Settings of Granitic Rocks. *Episodes*, **19**, 120-125. https://doi.org/10.18814/epiiugs/1996/v19i4/005